Tensile Properties of Fiber Reinforced Concrete

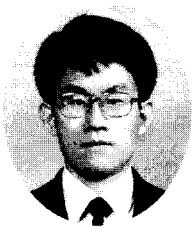
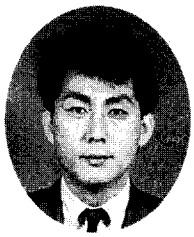


Cho, Baik-Soon* Back, Sung-Yong** Park, Hyun-Jung***

Abstract

Potentially significant mechanical improvements in tension can be achieved by the incorporation of randomly distributed, short discrete fibers in concrete. The improvements due to the incorporation fibers significantly influence the composite stress - strain (σ–ε) characteristics. In general incorporating fibers in a plain concrete has relatively small effect on its pre-cracking behavior. It, however, alters its post-cracking behavior quite significantly, resulting in greatly improved ductility, crack controls, and energy absorption capacity (or toughness). Therefore, a thorough understanding the complete tensile stress - strain (σ–ε) response of fiber reinforced concrete is necessary for proper analysis while using structural components made with fiber reinforced concrete.

Direct tensile stress applied to a specimen is in principle the simplest configuration for determining the tensile response of concrete. However, problems associated with testing brittle materials in tension include (i) the problem related to gripping of the specimen and (ii) the problem of ensuring centric loading. Routinely, indirect tension tests for plain concrete, flexural and split-cylinder tests, have been used as simpler alternatives to direct uniaxial tension test. They are assumed to suitable for fiber reinforced concrete since typically such composites comprise 98% by volume of plain concrete. Clearly since the post-cracking characteristics are significantly influenced by the reinforcing parameters and interface characteristics, it would be fundamentally incorrect to use indirect tensile tests for determining the tensile properties of fiber reinforced concrete. The present investigation represents a systematic look at the failure and toughening mechanisms and macroscopic stress - strain (σ–ε) characteristics of fiber reinforced concrete in the uniaxial tension test. Results from an experimental parametric study involving used fiber quantity, type, and mechanical properties in the uniaxial tension test are presented and discussed.

Keywords : fiber reinforced concrete, uniaxial tension test, steel fibers, polypropylene fibers, toughness, energy absorption capacity

* KCI Member, Assistant Professor, Department of Civil Engineering, Inje University, Korea.
** Associate Professor, Department of Civil Engineering, Inje University, Korea.
*** Graduate Student, Department of Architectural Engineering, Pusan National University, Korea.

1. Introduction

Concrete is one of the most commonly used materials in structural applications. It has adequate compressive strength and stiffness. However, it has low tensile strength and low ductility resulting in low energy absorption. Due to its lack of tensile strength and ductility, concrete is often reinforced with reinforcing steel bars and entire tensile forces are assumed to be carried by the reinforced steel bars. Such applications under abusive environmental conditions often result in corrosion of the steel rebars, and consequently affect the decay of reinforced concrete structures adversely.

An intrinsic cause of the poor tensile behavior of concrete is its low toughness and the presence of defects. Therefore, improving concrete toughness and reducing the size and number of defects in concrete would lead to better performance. An effective way to improve the toughness of concrete is by adding a small fraction (usually below 2% by volume) of short fibers to the concrete during mixing. In the fracture process of fiber reinforced concrete (FRC), fibers bridging the cracks in the matrix can provide resistance to crack propagation and crack opening before being pulled-out or stressed to rupture. After extensive studies in the last three decades, it is now beyond doubt that such fiber reinforcement can improve the tensile properties of concrete[14]. Orders of magnitude increase in ductility (energy absorption capacity) over plain concrete is commonly observed. Improved fatigue strength and reduced drying shrinkage are also often observed[4]. Fiber reinforced concrete is currently being used in many applications including highway overlays, bridges, airport runways and buildings [2,5,10]. In load bearing applications it is generally used along with traditional steel reinforcement[1].

Direct tensile stress applied to a specimen is in principle the simplest configuration for determining the tensile response of concrete. However, problems associated with testing brittle materials in tension[7,8,15] include (i) the problem related to gripping of the specimen – failure of the specimen at or near the grips results from stress concentrations at these locations and (ii) the problem of ensuring centric loading – even if one takes great care the loading is typically eccentric. Additionally once the specimen cracks on one side, locally, the loading at the critical section is still eccentric even if one assures that the external loading is truly uniaxial. Routinely, indirect tension tests for plain concrete, flexural and split-cylinder tests, have been used as simpler alternatives to direct uniaxial tension test. They are assumed to suitable for FRC since typically such composites comprise 98% by volume of plain concrete. Clearly since the post-cracking characteristics are significantly influenced by the reinforcing parameters and interface characteristics, it would be fundamentally incorrect to use indirect tensile tests for FRC. The present investigation represents a systematic look at the failure and toughening mechanisms and macroscopic stress - strain (σ–ε) characteristics of FRC in the uniaxial tension test. Observation on an experimental study on the amount of fiber quantity, type, and mechanical properties in the uniaxial tension test are presented and discussed.

2. Experimental Program

The focus of this study was to investigate the effects of the type of fiber, geometry of the fiber, and fiber volume content on the overall tensile behavior of FRC. Of particular interest was the influence of these parameters on its tensile strength and energy absorption capacity in uniaxial tension test. Based on the type of fiber, fiber geometry, and fiber volume content of interest, the experimental program included eight

mixes. Two types of steel fibers (volume fractions of 0.5% and 1.0%) and two types of fibrillated polypropylene fibers (volume fractions of 0.1% and 0.5%) were used.

2.1 Specimen Preparation

The eight matrix mixes used for this investigation were designed for approximate 28 day compressive strengths of 350 to 420 kgf/cm^2. Type I Ordinary Portland Cement was used. Washed river sand was used as fine aggregates and crushed limestone having maximum size of 19mm was used as coarse aggregates. All aggregates used met ASTM C33 specifications. Superplasticizer was used to achieve the required level of workability. On the recommendation of polypropylene 2 type fiber manufacturer, superplasticizer was not added. In order to achieve equivalent levels of workability the water-cement ratio and the sand-coarse aggregate ratio were increased in these mixes. Air entraining agent was used to produce air contents of between 5 to 7%. Details of the mix proportions are presented in Table 1.

A large slab (15.2cm deep, 5.29m x 1.22m) was cast for each of the eight mixes. The concrete truck placed the mix directly into the slab. A large slab was chosen so that specimens fabricated for future studies could be used. The slabs were left in the outdoor casting bed covered with polyethylene sheet for four days. After that, they were sawn into smaller sized slabs in order to facilitate further handling: 0.53m x 0.47m. The smaller slabs were stored in a curing room (approximately 98% R.H. and 24°C) until they were ready to be sawed into testing specimens. Then, the uniaxial tension specimens were sawed using a water-cooled masonry saw that was equipped with a 45.7cm diamond tipped circular blade with 3.2mm thickness. Notches were sawed using the same saw. Detailed specimen size is shown in Fig. 1. Slumps of all eight matrix mixes in the 8.9 to 14.0cm range were obtained.

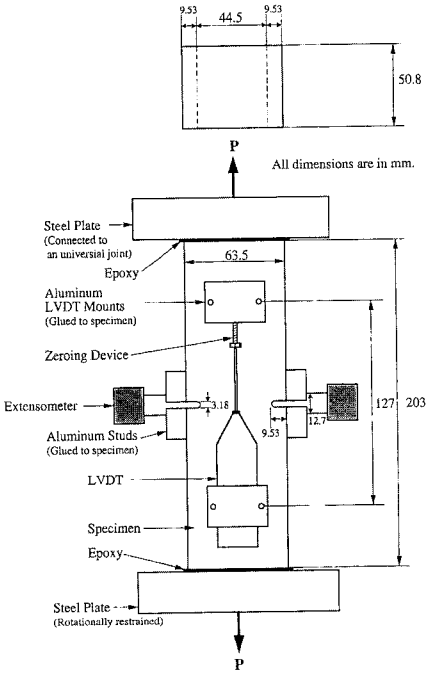

Fig. 1 Specimen loading and displacement measuring fixtures

Table 1 Typical mix proportion used

Constituent	All Mixes except Polypropylene 2 Mixes Content per cubic meter of concrete (m^3)	Polypropylene 2 Mixes Content per cubic meter of concrete (m^3)
Cement	277 kg	277 kg
Fine aggregate	644 kg	736 kg
Coarse aggregate	644 kg	510 kg
Water	138 kg	160 kg
Superplasticizer	532 cc	
Air-entraining agent	127 cc	127 cc

The steel fiber mixes had an average unit weight of 2.22 t/m^3 and the polypropylene fiber mixes had an average unit weight of 2.21 t/m^3.

2.2 Fibers

Two types of steel fibers and two types of fibrillated polypropylene fibers were used in this investigation. Steel fibers are typically used because of their high modulus of elasticity (2.0x10^6 kgf/cm^2) and polypropylene fibers are typically used because of their high ultimate elongation capacity (25%) and high tensile strength (4,900 - 5,600 kgf/cm^2) in spite of their low modulus of elasticity (49,000 - 81,200 kgf/cm^2). The hooked-end steel fibers were available in collated bundles. The fibers separate due to the mechanical action during mixing and due to the solubility of the glue. They were nominally 51mm long and had an effective aspect ratio of 100. The crimped steel fibers were also nominally 51mm long. They had a crescent-shaped cross-section and an equivalent aspect ratio of 50. Hooked-end steel fibers and crimped steel fibers were used in this investigation because of their improved resistance to pull-out compared to smooth straight fibers. Two polypropylene fibers used were of the fibrillated variety. During the mixing process, the fibrillated fibers typically break-up into individual fibrils. Since polypropylene fibers used were of the fibrillated type and not of the monofilament type it is inappropriate to compute and report equivalent diameters. Both the polypropylene fibers were also nominally 51mm long. The mechanical properties of the fibers used are listed in Table 2.

3. Test Procedure

The uniaxial tension test FRC specimens were 203mm long, 64mm wide, and 51mm thick. Symmetrical double edge notches were sawed for all the specimens (9.5mm deep and 3.2mm wide). The notches ensured both a predetermined crack location as well as stability in the "strain-controlled" test on MTS closed-loop testing machine. Specimen ends were glued to steel plates (127mm x 127mm x 25mm) using a room-temperature curing epoxy. Aluminum studs (15.9mm x 19.1 mm x 12.7mm) were glued across the notches to mount extensometers on the left and right faces of the specimen. Details of specimen loading and displacement measuring fixtures are illustrated in Fig. 1. The uniaxial tension test was conducted under specimen displacement controlled, strain-controlled, conditions (average of notch mouth opening displacement as measured using the two extensometers). All specimens were tested monotonically using an average notch mouth opening displacement rate of 0.013mm/sec (1 μstrain/sec). Each test lasted approximately 50 minutes. Load, average notch mouth opening displacement (12.7mm gage-length using two extensometers, specimen displacements measured over a longer gage-length (127mm gage-length) using two LVDTs, command signal, ram displacement and time (from the start of the test) were the parameters monitored during the test. A detailed schematic expression is shown in Fig. 2. A PC-based automated test control and data acquisition system was used for controlling the test as well as for acquiring data from the test.

Table 2 Mechanical properties of the fibers used

Fiber type	Tensile strength (σ, kgf/cm^2)	Modulus of elasticity (E, kgf/cm^2)	Specific gravity (ρ)
Hooked-end steel	11,900	2.0x10^6	7.85
Crimped steel	11,550	2.0x10^6	7.85
Polypropylene 1	4,900	49,000	0.91
Polypropylene 2	5,600	81,200	0.90

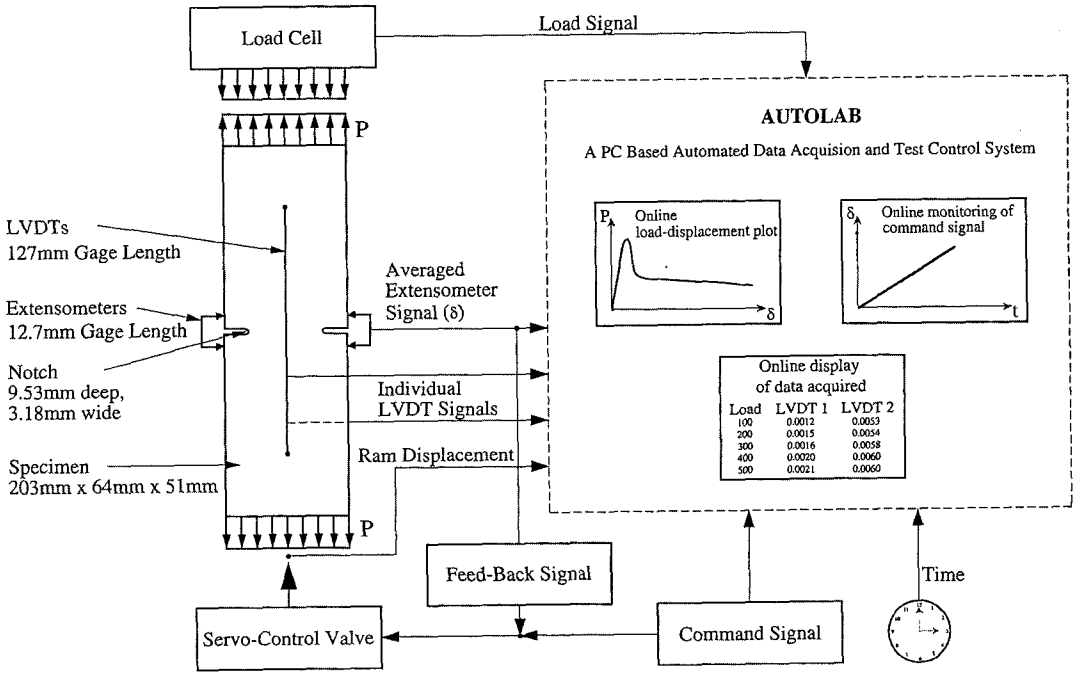

Fig. 2 Block diagram highlighting details of the closed-loop test scheme and associated instrumentation used for uniaxial tension test

4. Test Results and Discussions

Uniaxial tension tests typically provide the most direct and fundamental response from a fracture mechanics point of view because of (i) their relatively simple state of stress (uniform and uniaxial) and (ii) failures in most applications primarily initiate due to Mode I type of fracture. However, the presence of notches is expected to introduce stress concentrations in the vicinity of the notch tips. The two edge notches were provided primarily to assure stable fracture. Average material properties obtained from the experiments are summarized in Tables 3 and 4.

Values reported in Table 3 include the stress at first crack and the corresponding strain (f_{cr}, ε_{cr}), the ultimate stress and the corresponding strain (f_u, ε_u), and the initial tangent modulus (E_t). It is noted that the stress values reported are calculated based on net area. Corresponding strain values reported are based on displacement measurements over the long gage length using LVDT (δ_l=127mm). The initial tangent modulus (E_t) is obtained from regression analysis of the slope of the stress-strain response up to load levels that approximately 50% of the composite strength.

Table 4 presents data on energy absorption capacities of the various mixes. Energy absorption is computed as the area under the stress - strain diagram. These values have been computed up to (i) the first crack strain ε_{cr}, A_1, (ii) 3 times of the first crack strain ε_{cr}, A_2, (iii) 5.5 times of the first crack strain ε_{cr}, A_3, and (iv) 10.5 times of the first crack strain ε_{cr}, A_4. According to the ASTM C1018 toughness definitions for flexural test the above strain limits were chosen.

Table 3 Summary of experimental results – strength, strain, and modulus

Mix Designation Fiber Type	V_f(%)	f_{cr} (kgf/cm^2)	f_u (kgf/cm^2)	$_{cr}$ (strain)	$_u$ (strain)	E_t (x10^6,kgf/cm^2)
Hooked-end	0.5	31.5	36.7	101.7	126.8	0.313
Hooked-end	1.0	35.0	39.9	99.7	130.9	0.342
Crimped	0.5	31.3	35.9	94.2	116.6	0.333
Crimped	1.0	33.5	38.1	105.2	126.8	0.319
Polypropylene 1	0.1	28.4	33.2	86.4	101.4	0.329
Polypropylene 1	0.5	29.8	35.1	92.5	116.4	0.323
Polypropylene 2	0.1	27.7	32.2	88.5	108.3	0.301
Polypropylene 2	0.5	28.2	33.5	92.0	110.3	0.319

Table 4 Summary of experimental results –absorbed energy

Mix Designation Fiber Type	V_f(%)	(x10^{-5},kgf/cm^2)	(x10^{-5},kgf/cm^2)	A_3 (x10^{-5},kgf/cm^2)	A_4 (x10^{-5},kgf/cm^2)
Hooked-end	0.5	160	634	999	1712
Hooked-end	1.0	232	713	1212	2162
Crimped	0.5	174	588	899	1470
Crimped	1.0	194	567	967	1813
Polypropylene 1	0.1	149	415	562	738
Polypropylene 1	0.5	137	513	756	1113
Polypropylene 2	0.1	133	404	575	816
Polypropylene 2	0.5	128	506	802	1266

It can be observed that the initial regime of stress-strain (σ-ε) response of FRC is elastic. Beyond loads that correspond to approximately 85% of the strength of the composite, preexisting microcracks that are distributed uniformly throughout the specimen begin to grow. This results in macroscopic nonlinear response. The growth of the microcracks may be accompanied by limited partial debonding along the fiber-matrix interfaces. Further loading produces coalescence of microcracks. In the vicinity of the composite peak one group of microcracks that have coalesced into a major crack becomes dominant and critical. It is speculated that this leads to localization of strain and resultant macroscopically observed phenomenon of softening. All other microcrack based crack systems gradually unload, as the critical section softens. This makes the strain measurement gage length dependent. The values of ε_{short} and ε_{long} in Fig. 3 measured using an average from the two extensometers having 12.7mm gage length and from the two LVDTs having 127mm gage length, respectively. At small deformations obtained strain is independent of gage length. At very large displacements (beyond the peak after displacements are localized), opening crack width in the notched region dominates strain measurement.

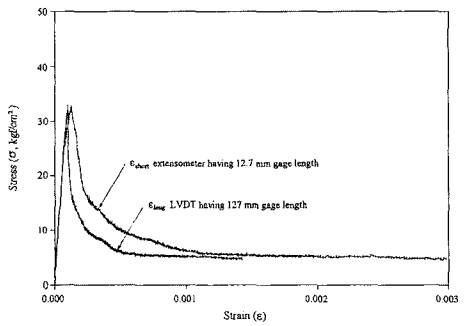

Fig. 3 Stress-strain response for polypropylene 1 reinforced mix with fiber volume fraction=0.1%

This effect can be observed in Fig. 3, which the stress–strain (σ-ε) responses obtained using two different gage lengths for fiber volume fraction of 0.1% polypropylene1 fiber reinforced mix.

Fig. 4 shows a comparison of the stress-strain response from mixes using different fiber types. Fiber volume fraction of 0.5% has been used for all the four plots. It can be observed that tensile strengths of the four mixes are somewhat different. The polypropylene mixes typically gave lower strengths even when the matrix used in each case was approximately the same strength. Moreover, the stress transferred in the post-crack regime is higher for the steel fibers. After the composite peak stress, the load-carrying capacity abruptly drops to a certain stress level termed by Naaman, et al.[12] as the postcracking strength. The mix containing hooked-end steel fiber absorbs the most energy. This followed by the mix containing crimped steel, polypropylene 2, and polypropylene 1. Although from Fig. 4 it appears that the postcracking response of all the four mixes are horizontal all of them indeed have a shallow negative slope. Frictional pull-out of fibers is perhaps largely responsible for this type of a response. The postcracking strength is fiber type dependent and varies between 70 to 140 kgf/cm^2 for the various FRC mixes used. They are approximately 20% to 40% of the composite strength.

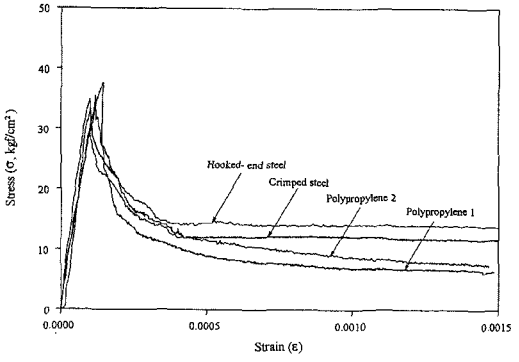

Fig. 4 Comparison of the typical stress-strain response for all the four fiber reinforced concrete mixes(fiber volume fraction = 0.5%)

Prior to cracking, the modulus of elasticity, E_t, of FRC composite can be obtained from the law of mixture, if there is perfect bond between the matrix and the fibers,

$$E_t = \alpha_1\alpha_2 E_f V_f + E_m V_m$$

where E_f and E_m are moduli of elasticity of fiber and matrix, respectively; V_f and V_m are the fiber and matrix volume fractions, respectively; α_1 and α_2 are efficiency factors for fiber orientation and for fiber length, respectively. It is obvious that α_1 is equal to 1 for fibers aligned in the direction of applied load. For randomly distributed fibers numerous articles reported a value of α_1, which depends on assumptions made in their analysis. According to Cox[6], α_1 can be estimated as 1/3 and 1/6 for two- and three-dimensional distributions, respectively. For continuous fibers α_2 is equal to 1. As the length of the fiber decreases within the matrix, its efficiency in carrying stress decreases since the fiber does not carry the same stress near its ends as its central portion does. Krenchel[11] has derived α_2 as 3/8 for randomly distributed discontinuous fibers in two-dimensional arrangement. Aveston et al.[3] have used a value of 1/2.

For concrete reinforced with steel fibers, the modulus of composite is expected to be greater than the modulus of unreinforced concrete, since modulus of steel is greater than modulus of concrete. For polypropylene fiber reinforced concrete, the modulus of composite is expected to be lesser than the modulus of unreinforced concrete, since modulus of polypropylene is lesser than modulus of concrete. Since the low fiber volume fraction (up to V_f=1%) was used in this investigation, it can be seen that the stiffness of FRC is not significantly affected by the fiber inclusion. This effect is plotted in Fig. 5 that the modulus of elasticity of the various FRC mixes used is insensitive to fiber type.

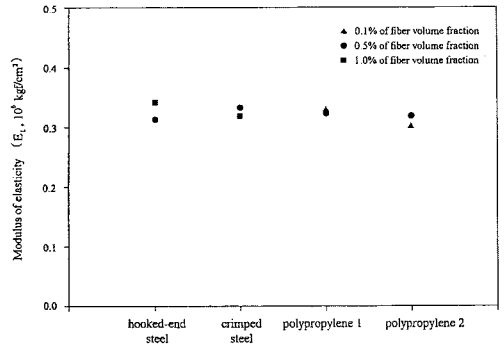

Fig. 5 Modulus of elasticity as a function of fiber type

Both the matrix and the fibers contribute to the tensile load-carrying capacity of the FRC composite. The ultimate tensile strength of FRC composite is somewhat sensitive to fiber reinforcement, as shown in Fig. 6. When a statistically significant set of data from other published sources[8,9] are added, as shown in Fig. 6, a clear trend of strength as related to the fiber reinforcement parameter (V_f l/d for steel fibers) becomes apparent. It can be stated that ultimate tensile strength of FRC is observed to be linearly related to the fiber reinforcement parameter.

The improvement of the energy absorption capacity of FRC is one of the primary reasons for adding fibers to concrete. Energy absorption has been computed as the area below the stress-strain

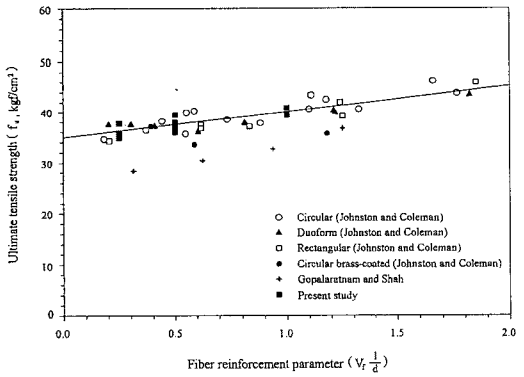

Fig. 6 Ultimate tensile as a function of the fiber reinforcement paramenter

curve. Absorbed energy for the various mixes tested are reported in Table 4. A comparison of the energy absorption capacity from mixes using different fiber types is illustrated in Fig. 7. Fiber volume fraction of 0.5% has been used for all four plots. Typically polypropylene reinforced mixes have a smaller energy absorption capacity compared to the steel fiber reinforced mixes. This can be attributed to the superior equivalent bond and higher stiffness in the latter mixes as compared to the former mixes. The mixes with hooked-end steel fibers have the largest energy absorption capacity. Increased energy absorption capacity makes the FRC composite attractive for use in applications where large amounts of energy absorption are required.

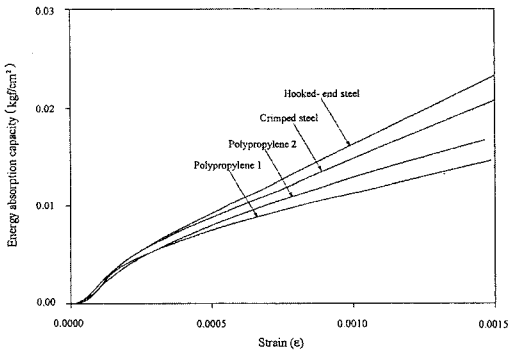

Fig. 7 Energy absorption capacity for all the four fiber reinforced concrete mixes (fiber volume fraction = 0.5%)

5. Conclusions

1. As a result of localization of displacements that begins to grow just prior to the peak stress, pre-cracking strain is independent of gage length. Whereas post-cracking strain is dependent of gage length since opening crack width in the notched region dominates strain measurement.
2. Modulus of elasticity of FRC (up to volume fraction of 1%) is matrix-dominated properties. It is not influenced significantly by the

fiber reinforcement parameters (fiber type, volume fraction, and aspect ratio). Whereas the ultimate tensile strength of FRC composite is somewhat sensitive to fiber reinforcement. When a statistically significant set of data from other published sources are added, a clear trend of strength as related to the fiber reinforcement parameter (V_f l/d for steel fibers) becomes apparent. It can be stated that ultimate tensile strength of FRC is observed to be linearly related to the fiber reinforcement parameter.

3. After the FRC composite peak stress, the load-carrying capacity abruptly drops to the postcracking strength. On further increases in displacement, the load carrying capacity gradually drops with a shallow negative slope. Frictional pull-out of fibers is perhaps largely responsible for this type of a response. This contributes to the improvement of the energy absorption capacity (or ductility). The postcracking strength is fiber type dependent and varies between 70 to 140 kgf/cm^2 for the various FRC mixes used.
4. The improvement of the energy absorption capacity (or ductility) of FRC is one of the primary reasons for adding fibers to concrete. Polypropylene reinforced mixes have a smaller energy absorption capacity compared to the steel fiber reinforced mixes. This can be attributed to the superior equivalent bond and higher stiffness in the latter mixes as compared to the former mixes. Increased energy absorption capacity makes the FRC composite attractive for use in applications where large amounts of energy absorption are required.

References

1. ACI Committee 544, "Design Consideration for Steel Fiber Reinforced Concrete," ACI Structural Journal, Vol. 85, No. 5, Nov.-Dec. 1988, pp. 563-580.
2. ACI Committee 544, "State-of-the-Art Report on Fiber Reinforced Concrete," ACI 544.1-96, American Concrete Institute, Detroit, 1996.
3. Aveston, J., Mercer, R. A., and Sillwood, J. M., "Fiber Reinforced Cements – Scientific foundation and Specifications," In Proceeding NPL Conference on Composites – Standards of Testing and Design, April 1974, IPC Science and Technology Press, Guildford, U. K., p. 93.
4. Balaguru, P. N. and Shah, S. P., "Fiber-Reinforced Cement Composites," McGraw-Hill, Inc., 1992.
5. Bentur, A. and Mindess, S., "Fiber Reinforced Cementitious Composites," Elsevier, London, 1990.
6. Cox, H. L., "The Elasticity and Strength of Paper and Other Fibrous Materials" British Journal of Applied Physics, Vol. 3, 1952, pp. 72-79.
7. Gopalaratnam, V. S. and Shah, S. P., "Softening Response of Plain Concrete in Direct Tension," ACI Journal, Vol. 82, No. 3, May-June 1985, pp. 310-323.
8. Gopalaratnam, V. S. and Shah, S. P., "Tensile Failure of Steel Fiber Reinforced Mortar," Journal of Engineering Mechanics, ASCE, Vol. 113, No. 5, May 1987, pp. 635-652.
9. Johnston, C. D. and Coleman, R. A., "Strength and Deformation of Steel Fiber Reinforced Mortar in Uniaxial Tension," Fiber-Reinforced Concrete, SP-44, American Concrete Institute, Detroit, 1974, pp. 177-193.
10. Keer, J. G. "New Reinforced Concrete: Concrete Technology and Design," Vol. 2, edited by R. N. Swamy, Surrey University Press, Blackie, London, 1984, pp. 52-105.
11. Krenchel, H., Fibre Reinforcement, Akademisk Forlag, Copenhagen, 1964, pp. 158.
12. Naaman, A. E., Moavenzadeh, F., and McGarry, F. J., "Probablistic Analysis of Fiber Reinforced Concrete," Journal of Engineering Mechanics, ASCE, Vol. 100, No. 2, April 1974, pp. 397-413.
13. Nielsen, L. E. and Chen, P. E., "Young's Modulus of Composites Filled with Randomly Oriented Fibers," Journal of Materials, Vol. 3, No. 2, 1968, pp. 352-358.
14. Shah, S. P., "Do Fibers Increase the Tensile Strength of Cement-Based Matrixes?," ACI Material Journal, Vol. 88, No. 6, Nov.-Dec. 1991, pp. 595-602.
15. Wang, Y., Li, V. C., and Backer, S., "Tensile Properties of Synthetic Fiber Reinforced Mortar," Cement and Concrete Composite, Vol. 12, 1990, pp. 29-40.